A Methodology for Analyzing Vibration Data from Planetary Gear Systems using Complex Morlet Wavelets

Abhinav Saxena, Biqing Wu, George Vachtsevanos
Department of Electrical and Computer Engineering, Georgia Institute of Technology, Atlanta
asaxena@ece.gatech.edu, becky.wu@ece.gatech.edu, gjv@ece.gatech.edu

Abstract

Planetary gear trains are complex flight critical components of helicopters and other aircraft. Failure modes on such components may lead to loss of life and/or aircraft. It is essential, therefore, that incipient failures or faults be detected and isolated as early as possible and corrective action be taken in order to avoid catastrophic events. Research thus far has focused on gear teeth faults and available methods could not detect a crack in the planetary gear plate under all operating conditions. A wavelet domain methodology is suggested for the analysis and feature extraction of the vibration data from the planetary gear system of military helicopters. Complex Morlet wavelets are employed and the time domain knowledge, preserved by the wavelet decomposition, is used to extract useful features that distinguish between faulted and healthy gear plates from experimental data made available from both on-aircraft and test cell experiments. A statistical method based on the z-test is also suggested to evaluate the relative performance of these features.

1. Introduction

The main transmission system composed of an epicyclic or planetary gear train ranks among the flight critical components of a helicopter. During the course of a typical flight it is subjected to sustained vibratory and impulsive loads often resulting in fatigue damage of its components. Thus, to ensure aircraft safety and reliability, frequent maintenance inspections, overhauls, and parts replacement must be carried out. This is an expensive and time consuming task, and hence a reliable damage detection technique is required. Research in recent years has focused on the development of vibration-based transmission fault detection techniques [2,6]. These techniques are applied to vibration signals collected from transducers, typically accelerometers, mounted onto the transmission housing. Externally mounted accelerometers result in the filtered response of the original vibration signal (through the transfer function of the housing) along with a significant noise contamination, making it more difficult for many signal processing techniques to detect the faults successfully, especially in the time domain. Thus the research has quickly expanded to include spectral, time-frequency and wavelet analyses for effective feature extraction.

The fault on the planetary gear is a crack in the carrier plate, and it is different from the usual tooth crack or breakage or from the faults in a fixed-axis gear, in which case various features based on the Time Synchronous Averaged (TSA) signal are sufficient to identify the fault. Such features are suitable for the faults associated with gear teeth and these features do not work very well for the planetary gearbox system as shown by [2]. Most of the multiple gear systems are analyzed based on TSA data. The TSA technique is intended to enhance the vibration frequencies that are multiples of the shaft frequency, which in many cases are related to the meshing of the gear teeth [3,4,5]. It is possible that the resonance frequency of the planetary gear that may indicate the plate crack fault is averaged out, since TSA tends to average out external disturbances and noise that are not in synch with the carrier rotation. In this paper a wavelet transform based methodology has been developed which clearly detects the transient dynamic phenomena emerging due to a cracked carrier plate.

2. Planetary gear data analysis

Rotorcraft transmission systems consist of an Epicyclic gear arrangement called planetary gear system (see Figure 2(a)). Such a system is defined by a sun/planet configuration, in which an inner “sun” gear is surrounded by two or more rotating “planet” gears, and a stationary outer ring gear. Torque is transmitted through the sun gear to the planets, which rides on a planetary carrier. The planetary carrier, in turn, transmits torque to the main rotor shaft and blades. Such systems are employed for high torque transmission requirements. Any fault occurring in this flight critical part can be catastrophic if not detected in time.

Recently two cracks of 10 inch and 3.25 inch in length were found in the planetary carrier of the main transmission gear of the U.S. Army’s UH-60A Blackhawk Helicopter [2]. Figure 2(b) shows the carrier

plate with a 3.25-inch crack detected during a maintenance operation. This resulted in flight restrictions on a significant number of the Army's UH-60A's. The planetary gear box is a complex system and a manual inspection of all 1000 transmissions is not only costly in terms of labor, but also time prohibitive. Therefore, it is extremely important to develop a simple, cost-effective test capable of diagnosing faults based on vibration data analysis.

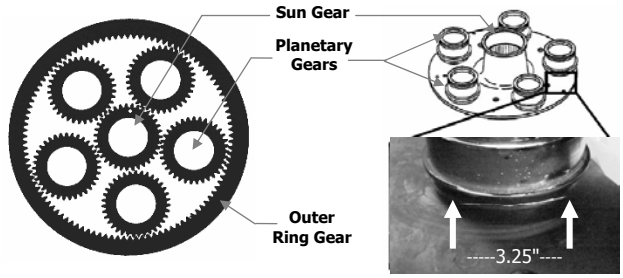

Figure 2. a) Planetary Gear Arrangement. b) Planetary gear plate crack

An integrated fault diagnostic/prognostic system architecture (Figure 3) has been developed for the Condition Based Maintenance (CBM) of critical military and industrial platforms [10].

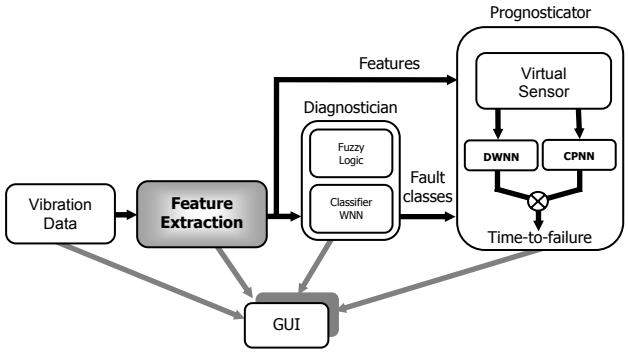

Figure 3. Integrated diagnosis/prognosis architecture for CBM

It consists of several modules integrating a number of functionalities. The success of this system in diagnosing and making predictions about remaining useful lifetime highly depends on the quality of features and hence the effectiveness of the feature extraction module. This paper describes an effective feature extraction technique based on wavelet analysis particularly for detecting the faults not associated with gear teeth which may not be detectable in gear mesh frequencies and TSA signals.

In order to generate test vibration data, measurements from the main transmission gear of the U.S. Army's UH-60A Blackhawk Helicopters were taken at the Helicopter Transmission Test facility (HTTF) at Patuxant River NAS, MD. The data was acquired using several sets of accelerometers employed in the US Army's Vibration Management Enhancement Program (VMEP) system. During a normal flight operation the transmission system undergoes a range of torque levels from 0% to 100%, hence it is important to consider the system dynamics at all torque levels. Since the transmission was not run for an extended period of time, only "snapshots" of data were recorded at six torque settings ranging from 20% to 100% in the test cell, and two torque settings at 20% and 30% on-aircraft [2]. Due to safety considerations, torque levels could not exceed 30% on aircraft tests. Each snapshot of the test cell data is 180 seconds long and was acquired at a rate of 100 kHz, and for on-aircraft data each snapshot is 25 seconds long and was acquired at a rate of 48 kHz. Tests under similar conditions were made for both healthy and faulted transmissions. Due to environmental conditions, the speed of the rotor does not remain perfectly constant and, therefore, a tachometer signal synchronized to the planetary gear plate is also included. Although several accelerometers were mounted at different locations (Figure 4), it was found that only two sensors, mounted on *PortRing* and *Input1* modules, provide important vibration signatures of the cracked carrier plate.

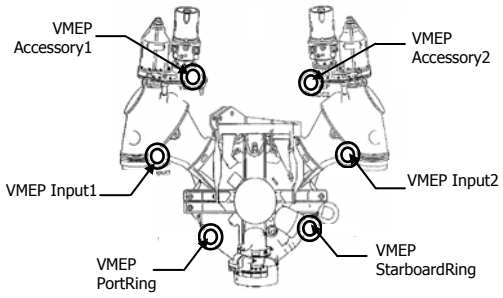

Figure 4. Location of the VMEP sensors on the main transmission

The majority of the data analysis techniques for gear systems are based on TSA of vibration signals [3,4,5]. As mentioned earlier, TSA based analysis is expected to reveal a fault associated with the gear tooth more effectively at the gear meshing frequencies, but for a fault like a crack on the plate this may not hold true. Instead , TSA may lead to undesirable averaging of some useful information for this kind of fault mode. Other studies based on the sidebands of the meshing frequencies in the TSA signal have not been very successful in detecting the faults [2,9]. The raw vibration signal instead of the TSA signal is used to extract the features since it provides better results as far as the available planetary gear data is concerned. Figure 5 shows the FFT spectrum for both TSA and raw vibration signals. It can be seen that raw data contains several non-mesh harmonic frequencies, with significant magnitudes as compared to mesh-

harmonics, which are absent in the TSA signal. Based on this observation, the wavelet investigation was focused on all the frequency ranges with dominant peaks in the FFT and not just the mesh harmonics.

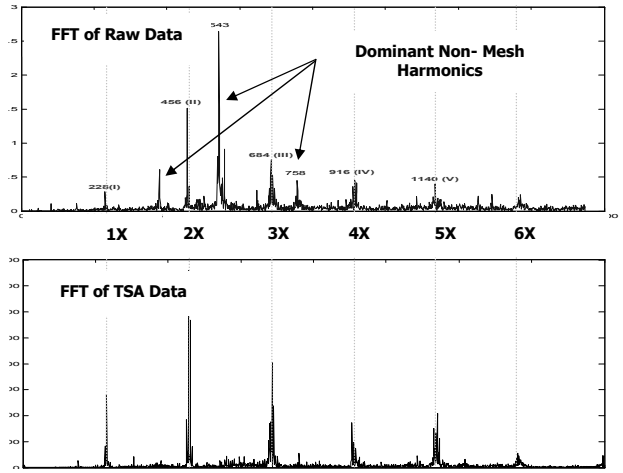

Figure 5. Comparing the FFT spectrum for raw data and TSA data

3. Wavelet methodology

The wavelet transform is a linear transform which uses a series of oscillating functions with different frequencies as window functions, $\psi_{\alpha,\beta}(t)$, to scan and translate the signal $x(t)$, where α is the dilation parameter for changing the oscillating frequency and β is the translation parameter. At high frequencies, the wavelet reaches a high time resolution but a low frequency resolution, whereas at low frequencies a low time and a high frequency resolution is achieved, which make them more suitable for non-stationary signal analysis. The basis function for the wavelet transform is given in terms of translation parameter β and dilation parameter α with the mother wavelet represented as:

$$\psi_{\alpha,\beta}(t) = \frac{1}{\sqrt{\alpha}}\psi\left(\frac{t-\beta}{\alpha}\right) \tag{1}$$

The wavelet transform, $W_{\psi}(\alpha,\beta)$, of a time signal $x(t)$ is given by:

$$W_{\psi}(\alpha,\beta) = \frac{1}{\sqrt{\alpha}}\int_{-\infty}^{+\infty} x(t)\psi^{*}\left(\frac{t-\beta}{\alpha}\right)dt \tag{2}$$

where $\psi^{*}(t)$ is the complex conjugate of $\psi(t)$. There are a number of different real and complex valued functions that can be used as analyzing wavelets. Morlet wavelets have been found to be among the most responsive wavelets to vibration signals. The complex Morlet wavelet is defined by Equation 3 in the time domain and by Equation 4 in frequency domain:

$$\psi_{Morlet}(t) = \frac{1}{\sqrt{\pi f_b}}\cdot e^{j2\pi f_c t-(t^2/f_b)} \tag{3}$$

$$\Psi_{Morlet}(f) = e^{\pi^2 f_b (f-f_c)^2} \tag{4}$$

Where f_c is the center frequency and f_b is the bandwidth (variance). Choosing a suitable combination of bandwidth and center frequency parameters is a design question, and depends on the signal under analysis. [8] describe a method to choose these parameters based on the sampling frequency of the signal and the number of sample points. Figure 6 shows the effect of the bandwidth parameter on Morlet wavelets in both the time and frequency domains. More mathematical details about Morlet wavelets and their properties with regard to their implementation can be found in [1,7].

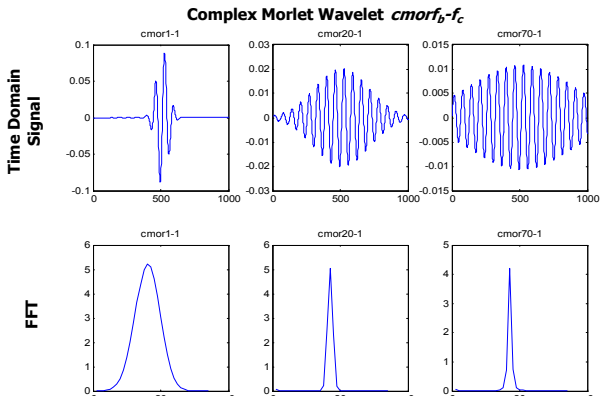

Figure 6. Complex Morlet wavelet with different bandwidth parameters

For the purpose of this study, the bandwidth and center frequency were experimentally determined to be 70 and 1 respectively, and hence the complex Morlet wavelet cmor70-1 (see Figure 1) was used for all the analysis steps. It was observed that the scalogram of one revolution data segment from the healthy transmission shows five distinct high energy areas corresponding to five different planets in the system (Figure 7). The energy is almost evenly distributed among all these areas. However, for the unhealthy transmission not only the energy distribution becomes asymmetric but also the relative magnitude of the energy increases. This forms the basis of the analysis using the wavelet transform. Three features were designed to describe these observations quantitatively. In order to describe the asymmetry developed within a single revolution, the wavelet map is divided into twenty equal segments and the energies of all these segments are calculated separately. The variance between these energies is calculated next and the temporal variance is expected to be higher for the unhealthy system due to the observed asymmetry.

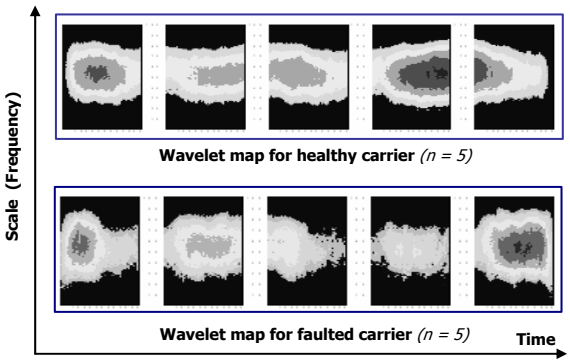

Figure 7. Energy distribution variation with time for both healthy and faulted carriers within one revolution. It becomes non-uniform within a revolution for the faulted carrier. Entire revolution has been divided into five equal segments to illustrate the difference in energy in various segments.

In order to account for an increase in the magnitude, two approaches are followed. For the overall increase in energy, the Frobenious Norm:

$$N_{frobenious} = diag\{\sqrt{C.C^T}\} \quad (6)$$

where C is any mxn matrix, is calculated for the wavelet coefficients in each of the twenty segments and their average is taken as a feature value for one complete revolution. The higher Frobenious Norm average suggests an increase in energy, and hence the presence of the fault. Also a higher value of the maximum energy among all the twenty segments is used as a feature suggesting an increase in energy as well as the asymmetry in the wavelet map. The results from the analysis are presented in the next section.

Effective fault diagnosis and prognosis is based on the quality of the features selected and extracted and thus feature performance evaluation forms an important part of the analysis. The features described above were calculated for all 720 revolutions of data. Feature values for 10 consecutive revolutions were averaged to get a more representative feature value in temporal domain. Thus, 72 points were obtained for each test carried out on the testcell and 10 points for the corresponding tests on the aircraft. The process was repeated for all torque settings on data from both healthy and faulted systems in the test cell as well as on-aircraft test conditions. A two sample z-test was conducted to statistically confirm that the clusters of the faulted and healthy systems form non-overlapping distributions. The z-test value is calculated as:

$$z = \frac{\overline{X}_1 - \overline{X}_2}{\sqrt{\frac{s_{X_1}^2}{n_1} + \frac{s_{X2}^2}{n_2}}} \quad (7)$$

$\overline{X}_1$ & $\overline{X}_2$ are the means of the feature values of faulted (1) and unfaulted (2) data segments. S_{X1} & S_{X2} are the standard deviations and n_1 & n_2 are the number of sample points in the respective distributions (e.g. 72 for testcell and 10 for aircraft tests).

4. Results and discussion

Three features based on the wavelet coefficients are calculated, as described in Section 3. Although the features calculated from several frequency bands perform well, only few are presented here [9]. The best results are obtained around the fifth harmonic (5x) for Input1 sensor and the tenth harmonic (10x) for the PortRing sensor. Each frequency band consists of ±20 Hz around the mesh harmonics, and therefore takes into account up to five sidebands appearing in the FFT spectrum. Figure 8(a) shows the three features evaluated on the PortRing sensor data from the test cell. It can be seen that the Frobenious norm forms the most compact clusters and, therefore, is the best in detecting and identifying the fault.

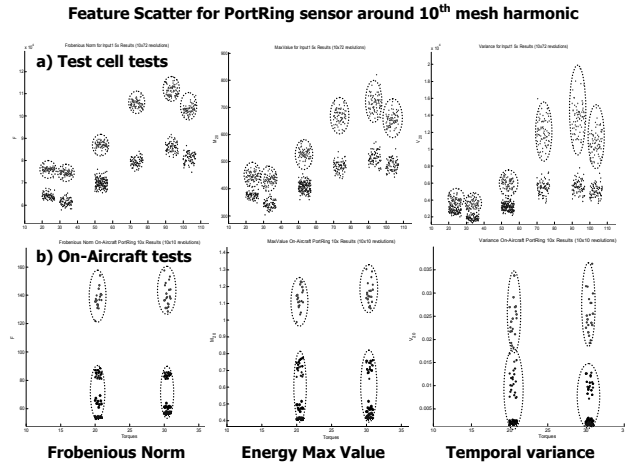

Figure 8. The three columns represent three features namely Frobenious Norm, Energy MaxValue and Temporal Variance in that order. (a) Features plotted for 6 different torque levels namely 20, 30, 50, 70, 90 and 100%. Top clusters represent the spread of faulted data and the bottom clusters represent healthy data. (b) Features for on-aircraft tests correspond to 20% and 30% torque values. The bottom clusters consist of 4 different experiments conducted on a healthy carrier.

The temporal variance also distinguishes the faulty carrier but the scatter between different revolutions is quite high and hence a lower confidence must be assigned to its accuracy. Especially at low torque values, the faulted data cluster is quite close to the healthy data even though they do not actually overlap. Similar conclusions can be drawn for the aircraft tests shown in Figure 8(b). For the aircraft, two sets of experimental data were available for the faulty carrier and four sets for the healthy carrier. Hence, the top

and bottom clusters actually consist of two and four clusters, respectively. Figures 9(a) and 9(b) show the results from the Input1 sensor for the same experiments. The observations made above also hold true in this case, but the clusters attain a much better separation in all cases, suggesting a more reliable performance as compared to the PortRing sensor. Another important observation is that no definite trend (increasing or decreasing) in the feature value variation is observed with varying torque. It was realized that some features work only at specific torque values and not over the complete range.

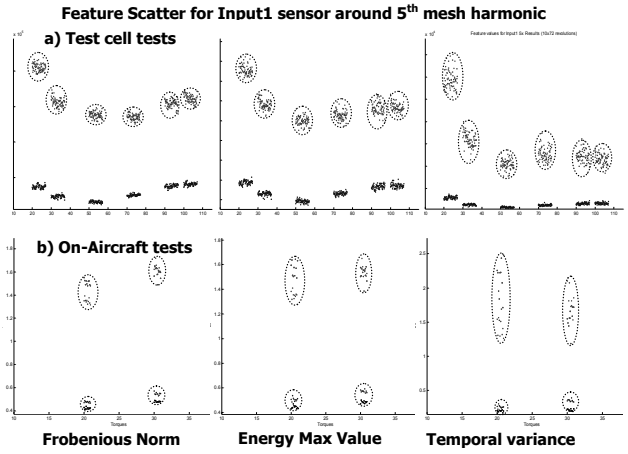

Figure 9. The three columns represent three features namely Frobenious Norm, Energy MaxValue and Temporal Variance in that order. (a) Features plotted for 6 different torque levels namely 20, 30, 50, 70, 90 and 100%. (b) Features for on-aircraft tests correspond to 20% and 30% in each case. A higher scatter in temporal variance can be seen in all the cases.

The effect of crack size and torque levels on these features needs to be understood and is under further investigation. For more effective diagnosis, different torque levels can be considered as separate operating modes and the features best suited to each operating mode can be used without even knowing the exact trend of the feature variation with varying torque values. This will additionally require information about the operating torque level which is easily available through torque measurements during the flights.

Feature Performance Evaluation: As discussed above, even though the three features distinguish between the faulted and the healthy data quite well, it is important to asses their relative performances [9]. As can be seen from Figures 8 and 9, the Frobenious norm appears to perform the best and the scatter in the temporal variance is the highest. But all of them can be important as they convey different information about the data. Thus, a 2-sample z-test was conducted to perform a relative assessment of the feature performance. The 2-sample z-test assesses whether the means of two groups are statistically different from each other, and thereby provides a useful tool to measure the distance between two distributions. Figures 10 and 11 show the relative z-test values. The higher the z-value the better is the feature. It is also clear that none of the features exhibit a consistent advantage over the others. One way to exploit this non-uniformity is to make the features complementary to each other and fuse them so as to improve the performance of a classifier. The integrated diagnosis/prognosis system mentioned above utilizes several techniques to fuse the information from several sources in order to generate an effective CBM schedule.

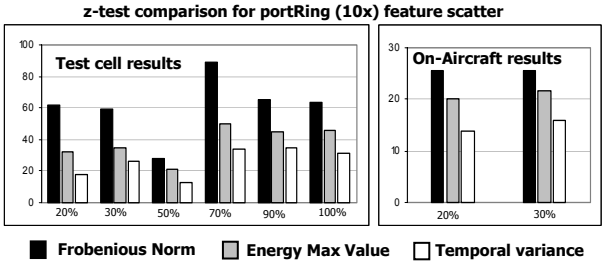

Figure 10. Z-test results for PortRing sensor

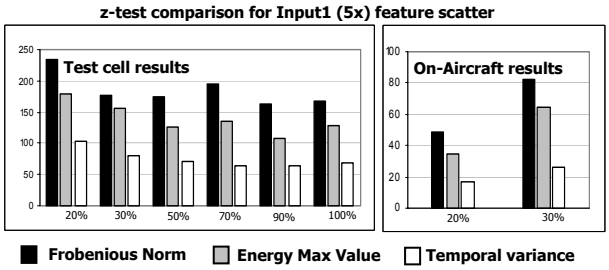

Figure 11. Z-test results for Input1 sensor

The success of the analysis based on raw signals as against the conventional TSA technique can be argued based on the hypothesis that the change in frequency content generated by the crack may not be harmonic with gear mesh frequencies and hence it is averaged out. There is also a possibility that the resonance frequencies of the planetary gear plate, which might be indicative of the plate crack fault, are averaged out since TSA tends to average out all external disturbances and noise that are not in synch with the carrier rotation. Some mesh harmonics and their sidebands can also be averaged out or reduced if their initial phases at the start of each carrier rotation are different. Further investigation is required to explain these observations and improve the results thereon.

5. Conclusions

It has been shown that the proposed wavelet domain methodology for the analysis and feature extraction of the vibration data from a planetary gear system of the Blackhawk helicopter has been successful in identifying the fault condition in all cases. In addition to the new feature extraction technique, a statistical method based on the z-test also suggests that, in terms of the relative performance of the features, the Frobenious Norm of the wavelet map is the best. But since the other two features convey important information about the time domain variations at specific frequency bands, they are also important. Further investigations are required based on new experiments to confirm the reliability of the method and to standardize the process for feature extraction. Several attempts are also being made to explain these observations via physical model-based techniques, which will be suitable for developing a real time prognostic system after successful fault diagnosis.

6. Acknowledgement

This work has been supported by the Defense Advanced Research Project Agency (DARPA), subcontract with Northrop Grumman Corporation under the program titled "Structural Integrity Prognosis System." The authors would like to thank Dr. Jonathan A. Keller of the U.S. Army AMCOM, Aviation Engineering Directorate at Redstone Arsenal, AL for providing the vibration data.

7. References

[1] ChongChun, L., Zhending, Q. (2000), "A Method Based on Morlet Wavelet for Extracting Vibration Signal Envelope", pp. 337-340.

[2] Keller, J., Grabill, P. (2003), "Vibration Monitoring of a UH-60A Main Transmission Planetary Carrier Fault," *the American Helicopter Society 59thAnnual Forum*, Phoenix, Arizona, May 6 –8.

[3] McClintic, K., Lebold, M.,Maynard, K., Byington, C., Campbell, R.(2000), "Residual and Difference Feature Analysis with Transitional Gearbox Data", *Proceedings of the 54th Meeting of the Society for Machinery Failure Prevention Technology*, Virginia Beach, VA, May 1-4, pp. 635-645.

[4] McFadden, P. D. (1991), "A technique for calculating the time domain averages of the vibration of the individual planet gears and sun gear in an epicyclic gearbox," *Journal of Sound and Vibration*, 144(1), pp. 163–172.

[5] McFadden, P.D. (1989), "Interpolation techniques for time domain averaging of gear vibration," *Mechanical Systems and Signal Processing*, 3(1), pp. 87–97.

[6] Samuel, P.D. (2003), "Helicopter Transmission Diagnostics Using Constrained Adaptive Lifting", *PhD. Thesis*, Department of Aerospace Engineering, University of Maryland College Park.

[7] Teolis, A. (1998), *Computational Signal Processing with Wavelets*, Birkhauser.

[8] Wang, G.F., Wang, T.Y., Ren C.Z., Li, H.W., Wang, X.B. (2004), "Application of Complex Shifted Morlet Wavelet in Vibration Monitoring of Spindle Bearing of Crank Shaft Grinder" *Key Engineering Materials*, vols. 259-260, pp. 697-701.

[9] Wu, B., Saxena, A., Khawaja, T.S., Patrick, R., Vachtsevanos, G. and Sparis, P. (2004), " An Approach to Fault Diagnosis of Helicopter Planetary Gears" to appear in *AUTOTESTCON 2004*, San Antonio, TX.

[10] Zhang, G., Lee, S., Propes, N., Zhao, Y., Vachtsevanos,G., Thakker., A., Galie, T., (2002), "A Novel Architecture for an Integrated fault Diagnostic/Prognostic System", *AAAI Symposium,* Stanford, California.